

## NUMERICAL SIMULATION STUDY OF AVALANCHES

By G. BRUGNOT

(Centre Technique du Génie Rural, des Eaux et des Forêts, Domaine Universitaire, B.P. 114,  
38402 Saint-Martin-d'Hères, France)

and R. POCHAT

(Centre Technique du Génie Rural, des Eaux et des Forêts, Parc de Tourvoie, 92160 Antony,  
France)

**ABSTRACT.** To provide engineers with a better tool, we have developed a program for avalanche computation. After a brief description of the mathematical model and the assumptions, we describe influence of physical and numerical parameters, which allows a better understanding of the physical phenomenon which we call an avalanche. The satisfactory agreement between computations and observations allows us to assume that the model is well founded; further experiments will allow us to improve this simulation tool.

**RÉSUMÉ.** *Simulation numérique des avalanches.* Pour donner aux ingénieurs un meilleur outil, nous avons développé un programme permettant le calcul des avalanches. Après une brève description du modèle mathématique et des hypothèses faites nous décrivons l'influence des paramètres numériques et physiques, ce qui permet une meilleure compréhension du phénomène physique qu'est l'avalanche. Une excellente concordance entre les calculs et les observations nous permet de conclure que le modèle est bien adapté. D'autres expériences nous mettront en mesure d'améliorer cet instrument de simulation.

**ZUSAMMENFASSUNG.** *Numerische Simulation von Lawinen.* Als Hilfe für ingenieurtechnische Massnahmen wurde ein Programm zur Berechnung von Lawinen entwickelt. Nach einer kurzen Beschreibung des mathematischen Modells und seiner Voraussetzungen wird der Einfluss physikalischer und numerischer Parameter behandelt, woraus sich ein klares Verständnis für den physikalischen Vorgang der Lawinenbildung ergibt. Die hinreichend gute Übereinstimmung zwischen Rechnung und Beobachtung weist auf die hohe Wirklichkeitsnähe des Modells hin. Durch weitere Versuche kann dieses Hilfsmittel der Simulation noch verbessert werden.

### 1. INTRODUCTION

It is becoming more and more evident that specific quantitative data must be available in order to characterize snow-avalanche phenomena. The growing urbanization of mountain areas is accompanied by intensified construction and interconnecting communication routes; as a result, a considerable number of people have been led to live and travel in avalanche-prone zones. In addition, formerly established villages where inhabitants used to accept a residual risk with fatalism, are now demanding that government bodies provide shelter from any danger.

In practical terms, the specialist must be able to answer two types of question. One requirement is determining the specific local area of risk, in other words defining the zones where there is no danger, which means a zone where avalanche action however minimal during a certain characteristic time period, which is represented by the period during which the climate is stable, is of negligible probability. A second requirement is the ability to estimate the overloads which a given "building" may be subjected to within the doubtful zone (this could refer to a bridge, roadway, "passive" protection structure, etc.).

The term "avalanche" is used to refer to a number of rather different kinds of snow flow. The ability to define a powder-snow avalanche, an aerosol consisting of snow which is pulverized in air (Hopfinger and Tochon-Danguy, 1977), is more or less established. As an extreme case, melted-snow avalanches consist of wet snow and are characterized by a quasi-laminar type flow. This type of avalanche is much slower and considerably more dense. As an intermediate case, and depending upon the original state of snow, we find complex flow, generally of a multi-strata nature, and composed of air and ice, characterized by varying degrees of turbulence, density, and velocity.

When confronted with an unexplored physical phenomenon, it is possible to consider two approaches—the analogical approach and the numerical approach. The first approach lends itself well to visualization and has enabled marked progress to be made in the field of powder-snow avalanches (Hopfinger and Tochon-Danguy, 1977) where engineers presently have interesting quantitative data at their disposal.

The second approach enables a high degree of flexibility in utilization due to the fact that it allows extensive analysis of the sensitivity to poorly defined parameters. We consider this approach to be particularly well adapted to the study of melted-snow avalanches and certainly useful in the case of other types of avalanche, provided that the role played by friction with ambient air is limited. We can associate this type of approach with the previous simplified models elaborated by Voellmy (1955) and Kozik (1962) which have been of great service.

Modern methods of calculation (Mahmood and Yevjevich, 1975) make it possible to envisage more complex numerical models which more closely define the physical reality being studied.

## 2. MATHEMATICAL MODEL

### 2.1. Description of an avalanche

A schematic representation of the reality being studied is necessary for mathematical modelling. Couloir geometry is defined by a series of cross-sections, in other words the intersections of planes which are perpendicular to the line of greatest slope with respect to terrain relief. That schematization (Fig. 1) allows us to represent a one-dimensional flow.

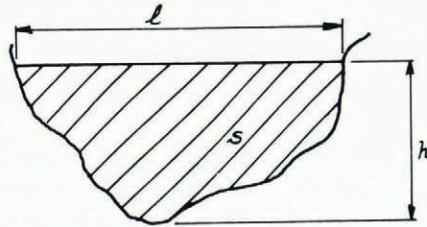


Fig. 1. Diagram showing schematic representation of couloir cross-section.

Let  $s$  be the wet area,  $l$  the width at the surface,  $h$  the snow depth, and  $R$  the hydraulic radius. Then in order at least partially to escape from the restrictions due to the indeterminate value of snow density  $\rho$  during flow, we consider the variables  $S = \rho s$  (units kg/m),  $H = \rho h$  (units kg/m<sup>2</sup>), and  $P = VS$  (units kg/s). The variable  $P$  represents snow flow rate;  $V$  is the average velocity of flow in the section parallel to the couloir axis. In such a model, we are not attempting to define the exact distribution of specific speeds at a given moment, as this would entail too much; we are calculating an average speed. Subsequent exploitation of our results requires that this be taken into account.

In addition, we have schematized the sections in the following theoretical form:

$$s = kh^n,$$

where  $k$  and  $n$  are variables along the couloir axis.

### 2.2. Hypotheses

We suppose the free surface to be horizontal in a cross-section and, connected with this, the distribution of pressures to be hydrostatic. These suppositions are an absolute requirement

for the derivation of simple equations. During flow, snow density varies as a function of snow speed and depth. As we do not know this law, we have tested the following form of variation:

$$\rho = \frac{\rho_0}{1 + \alpha(V - V_0)},$$

where  $\rho_0$  is the density at rest,  $V_0$  the threshold speed at which  $\rho$  varies, and  $\alpha$  the coefficient of variation. This obviously questionable law was introduced to attempt to quantify the influence of density.

Friction is represented in the form of a polynomial in  $V$ :  $F_p = f_s + f_1V + f_tV^2$  in which the three terms traditionally represent static friction, laminar friction, and turbulent friction. The coefficients of friction are selected on an *a priori* basis as a function of couloir roughness and geometry.

### 2.3. Equations

Flow equations for snow can be established by simple balance considerations. Conservation of the snow mass in motion requires

$$\frac{\partial S}{\partial t} + \frac{\partial P}{\partial x} = 0.$$

The momentum equation can be written

$$\begin{aligned} \frac{\partial P}{\partial t} - \frac{2P}{S} \frac{\partial S}{\partial t} + \left[ \frac{gh}{n} - \frac{P^2}{S^2} \right] \frac{\partial S}{\partial x} &= gS \sin \psi + \frac{gh}{n} \left( \frac{\partial S}{\partial x} \right) h \\ &= \text{const} - \left[ f_s g S \cos \psi + f_l g \frac{P}{R^2} + f_t g \frac{P^2}{SR} \right]. \end{aligned}$$

These equations apply to the entire flow with the exception of the frontal zone, for which we use equations of the "mobile jump" type; continuity implies

$$W(S - S_0) = P,$$

and dynamics give

$$P(W - V) = \frac{g}{n+1} (Sh - S_0 h_0),$$

where  $W$  is the advance velocity of the avalanche front and  $S_0$  the entrainment of existing snow by flow at the front level. The dynamic equation is obtained by means of a supplementary hypothesis being that pressure forces are preponderant and that friction at the bank as well as gravity in the frontal zone do not have to be taken into consideration. Eliminating  $W$  between the two front equations gives an equation  $F(P, S) = 0$  which can be used as a boundary condition for up-stream flow. Front velocity  $W$  is computed using the continuity equation after solving the flow equations.

### 2.4. Boundary conditions—initial conditions

Activation of flow when the avalanche starts is calculated by a mass-balance equation and an approximation of velocity. The free surface, in fact, is not horizontal in the section of the avalanche at its origin. On the other hand, as soon as there is a question of motion, this hypothesis becomes valid. Total snow mass, therefore, is considered with the context of motion applied (surface area of the point of origin times average depth of snow times apparent density of in-place snow) and snow depth is calculated for each flow cross-section in order to conserve this mass. The Voellmy formula is used to approximate velocity. The variability of initial conditions has little relevance to the following stages of the calculation, provided that the mass-balance equation is respected.

The phenomenon of snow entrainment up-stream of the avalanche front is not well known, and the mathematical model elaborated schematizes this recovery with the supposition that a given snow depth  $h_0$  (provided by the user in each section) is completely recovered at the avalanche front level (Fig. 2, diagram ①).

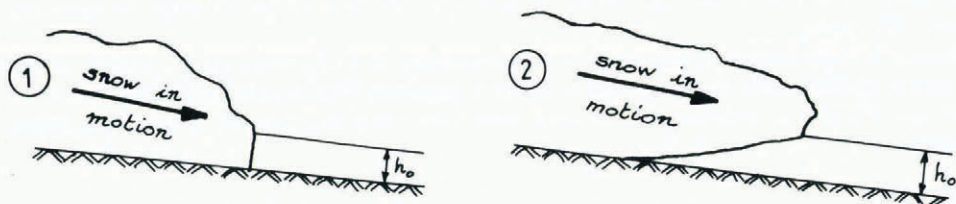


Fig. 2. Method of entrainment of snow by avalanche front assumed in the model (left) and as it is thought to occur in physical reality (right).

Actual entrainment is more probably gradual, in other words, partial recovery at the avalanche front level followed by recovery through the action of the snow in motion (Fig. 2, diagram ②). Through the intermediary of equations expressing the front, this recovery represents the down-stream limit condition of the model. We consider snow flow rate to be zero up-stream.

### 2.5. Solution

For solution of the system of partial differential equations we have selected a method using finite differences with an implicit solution. This type of method is commonly used in the mechanics of fluids. It allows us to calculate the progression of the variables  $S$  and  $P$  at each point in time. For a simulation, the computer program requires 16 000 words, 1.5 min using an Iris 80 (C II) computer, which represents a total cost of approximately 75 F.Fr. This limited cost makes it possible to perform any simulations required using different coefficient values and snow-data elements.

## 3. APPLICATIONS

### 3.1. Sensitivity analysis

In order to test how the model functions and the influence of the various hypotheses, we have conducted several simulations which make it possible to isolate the fundamental ideas required for comprehension of avalanche phenomena. The values of the coefficients used and of the geometry are given in Tables I and II respectively.

#### Friction

Figures 3 and 4 clearly show that, depending on the value selected, the model can give extremely varied results. The approach based on expressing friction in terms of a polynomial necessitates a setting of three coefficients and therefore the obligation to develop experience through comparison with observations. We consider this to be indispensable, and clearly Figure 1 demonstrates the influence of static friction on avalanche advance, which tends to prove that the period of time during which the snow is driven at high velocity (at a given abscissa) is limited in relation to the duration of flow. Figure 2 demonstrates the high degree of sensitivity obtained with the value assigned to the turbulent friction coefficient  $f_t$  for the velocity of advance of the front.

TABLE I. VALUES OF COEFFICIENTS

<i>Avalanche No.</i>	$f_s$	$f$	$10^3 f_a$	$\alpha$	<i>Entrainment h</i> m
1	0.2	0	5	0	0.05
2	0.2*	0	5	0	0.05
3	0.2†	0	5	0	0.05
4	0.2*	0	30	0	0.05
5	0.2*	0	15	0	0.05
6	0.2*	0	5	0	0.05
7	0.2*	0	5	0	0.05
8	0.2*	0	5	0.1	0.05
9	0.2*	0	5	0.3	0.05
10	0.2*	0	5	0.6	0.05
11	0.2*	0	5	0.3‡	0.05
12	0.2*	0	5	0.3	0.05
13	0.2*	0	5	0.3	0.05
14	0.2*	0	5	0.1	2
15	0.2*	0	5	0.1	0.05
16	0.2*	0	5	0.1	2 §
17	0.2*	0	5	0.1	2 §
18	0.2*	0	5	0.1	0.05 §

\* Or 0 if  $V > 3$ .  
 † Or 0 if  $V > 6$ .  
 ‡  $V_0 = 0.6$ .  
 § Then 3.

TABLE II. GEOMETRY

Maximal height of starting zone: 790 m  
 Minimal height of run-out zone: 340 m  
 Inclination of starting zone: 32.5°  
 Average inclination of avalanche path: 23.5°  
 Area of starting zone:  $1.3 \times 10^4 \text{ m}^2$   
 Length of starting zone: 205 m  
 Depth of snow in the starting zone: 1.5 m  
 Density of snow in the starting zone: 360 kg/m<sup>3</sup>

These figures make it possible to prove that overall flow factors determine front velocity, which clearly establishes the value of complete simulation models. The static friction coefficient and depth of recovery largely determine avalanche stopping.

*Apparent density*

Model sensitivity (Fig. 5) is not as distinctive as with friction. In reference to observations, we consider it reasonable to apply an “avalanche no. 11” type law to represent this phenomenon.

*Geometry variations*

When the couloir widens abruptly, flow obviously does not strictly follow the banks. By analogy with hydraulic flow, we restrict widening to 15° angles in the form given in Figure 6; beyond this limit equations are no longer valid. It should be noted, however (Fig. 7), that an abrupt widening (avalanche no. 12) results in a sudden braking of avalanche advance. Widening and narrowings of the couloir slow down the advance of the avalanche front, but do not have much effect on avalanche velocity itself. As a result, it appears that variable geometry cannot be relied upon to restrict avalanche advance. For this purpose, breaks in slope are much more efficient.

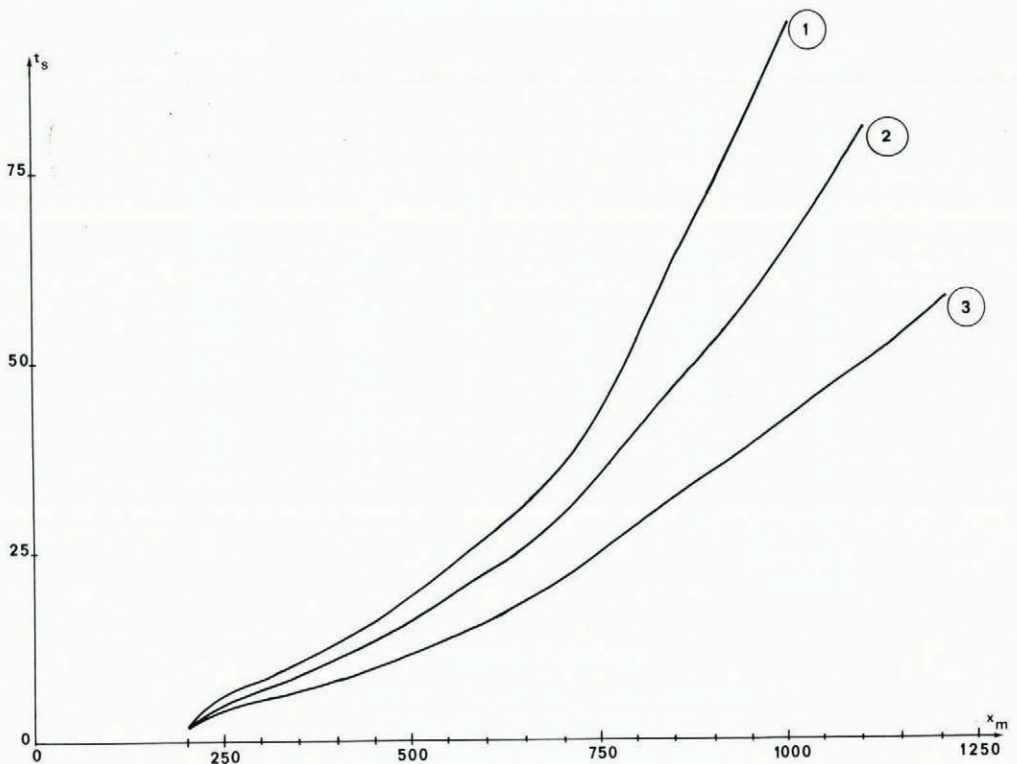


Fig. 3. Influence of static friction coefficient  $f_s$  on the flow curve of an avalanche. For avalanche 1,  $f_s = 0.2$ . For avalanche 2 it falls to zero if  $v > 3$  m/s. For avalanche 3 it falls to zero if  $v > 6$  m/s.

#### Depth of entrainment

Insufficient knowledge of the stresses involved in contact between the avalanche and in-place snow, as well as the relation between the entrainment and the value of these stresses, have not enabled us to build a mathematical model representing this phenomenon. Avalanches 14 (2 m of entrainment) and 15 (5 m of entrainment) emphasize the importance of this parameter (Fig. 8). For a considerable entrainment, the avalanche is slower at the outset due to more energy being required to set the snow into motion, then it is launched and acquires a much higher speed. In addition to this, the extent of entrainment largely determines the zone in which the avalanche stops and consequently the localization of avalanches.

#### Avalanche stopping

There are two problematical elements with respect to avalanche stopping; the first is description of the flow: when an avalanche reaches a widened zone, it does not generally spread out over the entire width, but divides up into forks, the localization of which can be observed on site. In this case, simulation consists in considering all or part of the avalanche, and limiting its impact to the width of the fork. This simulation can be performed for any advisable hypotheses. The second difficulty resides in modelling how the avalanche stops itself; to do this we compare the forces in such a way that an inverse relationship is obtained; as soon as the force due to static friction exceeds the sum of the forces due to inertia, pressure, and gravity, the avalanche is stopped.

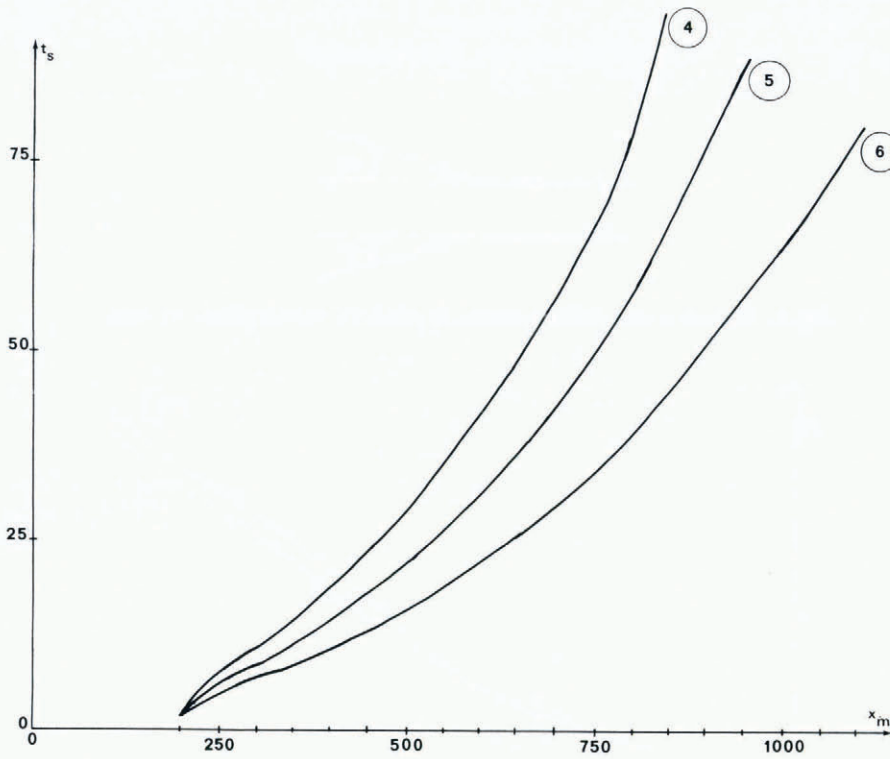


Fig. 4. Influence of the turbulent friction coefficient  $f_d$  on the flow curve of an avalanche. For avalanche 4,  $f_d = 30 \times 10^{-3}$ . For avalanche 5,  $f_d = 15 \times 10^{-3}$ . For avalanche 6,  $f_d = 5 \times 10^{-3}$ .

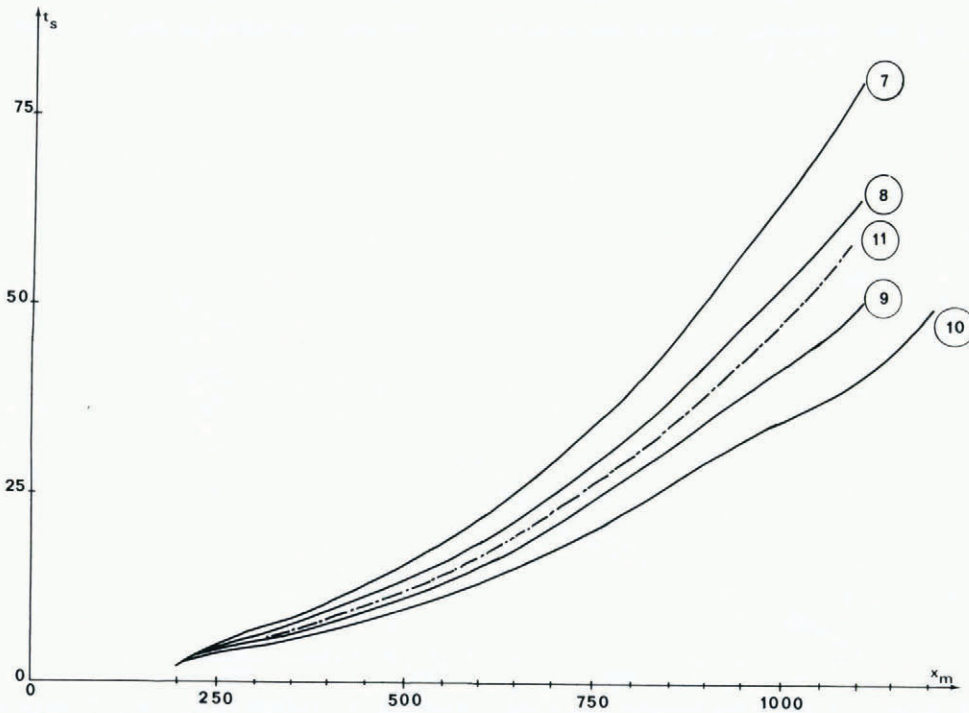


Fig. 5. Influence of the coefficient of variation of apparent density  $\alpha$  on the flow curve of an avalanche. For avalanche 7,  $\alpha = 0$ . For avalanche 8,  $\alpha = 0.1$ . For avalanches 9 and 11,  $\alpha = 0.3$ . For avalanches 10,  $\alpha = 0.5$ . In all cases except avalanche 11,  $V_0 = 0$ , and for avalanche 11,  $V_0 = 6$  m/s.

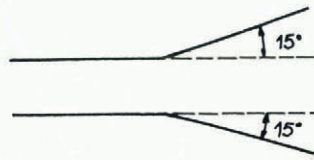


Fig. 6. Diagram to show limiting widening for which the avalanche follows the banks.

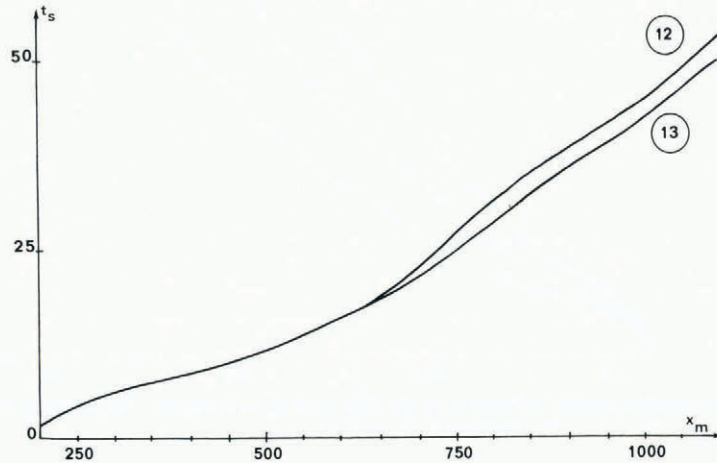


Fig. 7. Influence of the widening on the flow curve of an avalanche. For avalanche 12, the widening is abrupt. For avalanche 13, the widening is progressive.

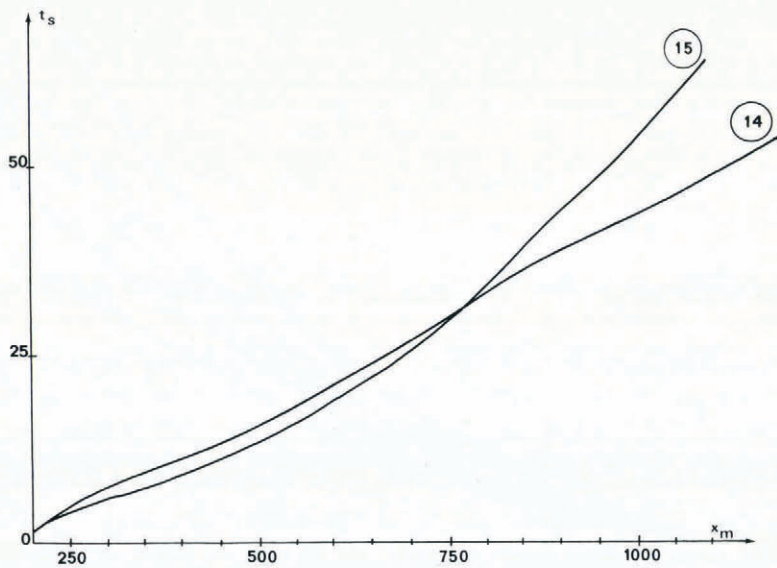


Fig. 8. Influence of the depth of entrainment on the flow curve of an avalanche. For avalanche 14,  $h_0 = 2$  m. For avalanche 15,  $h_0 = 0.05$  m.

Figure 9 shows avalanche stopping for three hypotheses about the depth of entrainment. A comparison of avalanches 16 and 17 show us how the stopping distance (avalanche 16, 100 m; avalanche 17, 40 m) is determined by flow inertia; the first case is slow ( $v \approx 5$  m/s) but the flowage represents a considerable mass; the second case is faster ( $v \approx 10$  m/s) and lower in mass, which results in rapid deceleration. Finally, these two avalanches stop at approximately the same point. Avalanche 18 is a more particular case: a sharp variation in depth of entrainment causes it to stop suddenly, and in this case, "the wall of snow" plays the role of a dam.

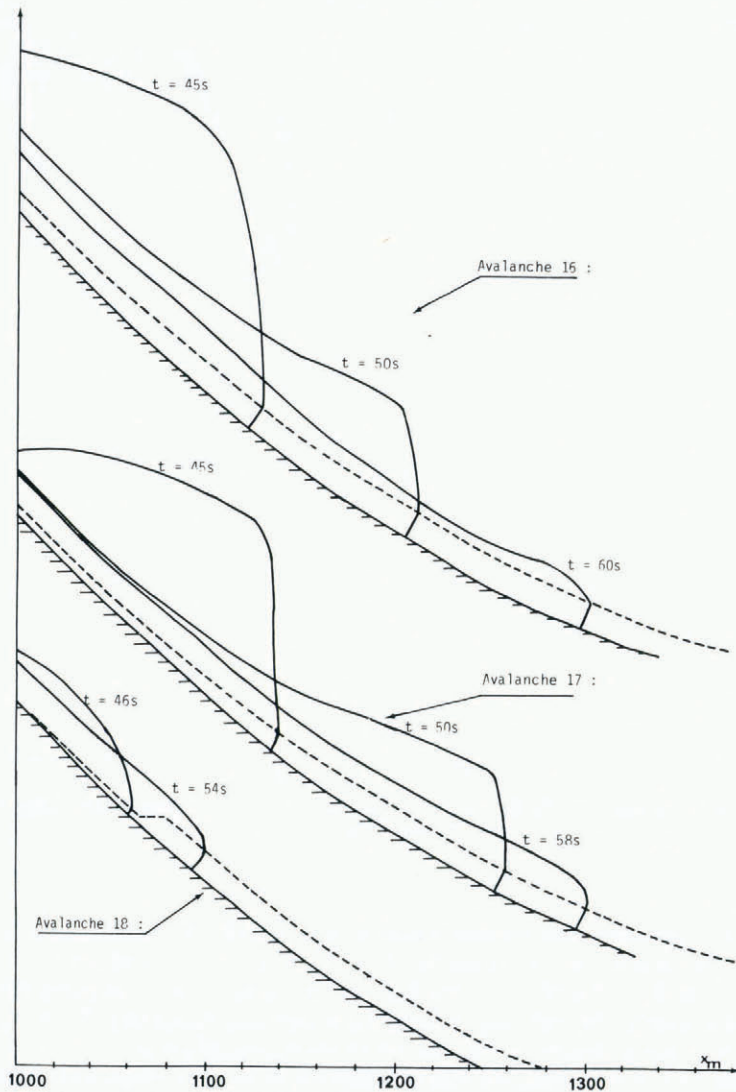


Fig. 9. Three cases of the termination of avalanches. Avalanche 16 encounters a progressive increase in the depth of entrainment up to  $h_0 = 3$  m at  $x = 1100$  m. Avalanche 17 has a much slower increase in the depth of entrainment up to  $h_0 = 3$  m at  $x = 1300$  m. Avalanche 18 encounters an abrupt increase in the depth of entrainment from  $h_0 = 0.05$  m to  $h_0 = 3$  m at  $x = 1060$  m.

### 3.2. Comparison with other models

We have compared the results obtained using this model with those of the simplified model elaborated by Voellmy (1955). Figures 10 and 11 demonstrate that in rigorous terms there is no correlation between slope, width, and avalanche front velocity.

Figure 10 enables a comparison to be made with the Voellmy formula; on the average the latter represents an avalanche front velocity value which is equivalent to the velocity observed. This formula, however, does not provide information on instantaneous velocities; in this case the formula for the avalanche in question contains a rate of error which can reach 60%.

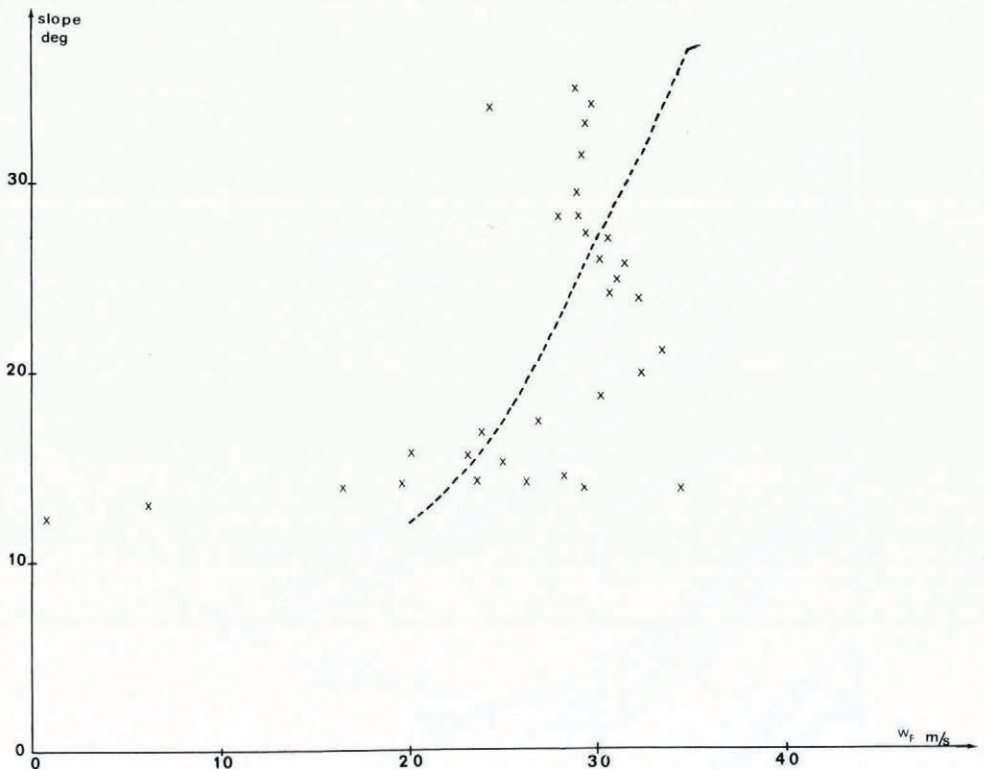


Fig. 10. Slope of ground plotted against velocity  $W_F$  of avalanche front. The relation predicted by Voellmy  $V = \sqrt{(\xi h \sin \alpha)}$  is plotted for  $h = 2000$  m, the mean value, as the dashed curve.

Figure 11 demonstrates that section width is not correlated to avalanche front velocity. The rectangle represented in the drawing designates a result obtained with the Voellmy formula, a variation in width of 50% which causes a variation in avalanche front velocity of approximately 15% only. In this way, a formula which only takes depth into account (shape being ignored) will not generate systematic and consequential errors.

Figures 10 and 11 clearly indicate that in addition to the two classical factors of slope and geometry which determine the velocity of advance of the avalanche front, a representation of the instantaneous velocities observed requires the elaboration of a complete model which takes slope, friction, inertia, and flow into account on a separate basis.

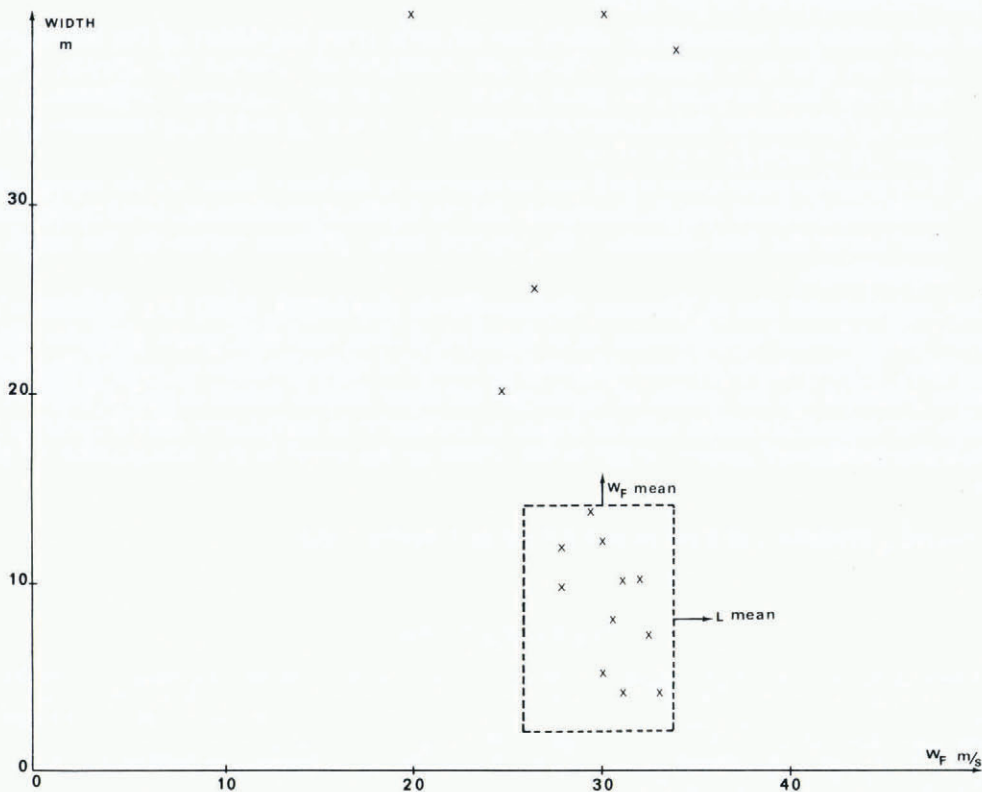


Fig. 11. Section width plotted against velocity  $W_F$  of avalanche front.

4. CONCLUSION

To verify how the model functions, we compared the experimental *in situ* Soviet results (Samoylov, 1976) with our calculations. The example which is of interest to us is relatively special: an initial avalanche which cleared out the entire couloir, followed by the activation of a second avalanche which spread over a very smooth surface without any entrainment up to the zone in which the first avalanche stopped.

Comparisons of experimental results with those of calculations has proven satisfactory, but a few major observations must be made:

- (i) The value for the instantaneous velocities of advance of the avalanche front is highly dependent on geometrical variations (for which global advance has limited response). However, data for these variations, are very scarce. Despite this, the rate of error remains below 15%.
- (ii) The value for front advance is quite satisfactory, which proves that we have not introduced any systematic errors in our calculation of instantaneous velocities.

As we have just witnessed, the flexibility of our numerical model is remarkable. This flexibility represents a certain danger due to the possibility of deviating widely from physical reality without our being clearly aware of it. It is fundamental to rely on experimentation in order to examine the equivalence between the model and reality. Only such experimentation will make it possible to “set” the numerous parameters gradually introduced to satisfy the requirements of establishing and solving the equations.

These parameters are of two types:

- (a) four numerical constants for which our relatively poor knowledge of the phenomena does not give us a measure. These are coefficient of variation for density, which influences front velocity; its value is near 0.1, and the roughness coefficients  $f_s$ ,  $f_l$ , and  $f_t$ ;  $f_s$  influences the avalanche stopping ( $f_s = 0.2$ );  $f_l$  and  $f_t$  can influence all the flow ( $f_l = 10^{-2}$ ;  $f_t = 5 \times 10^{-3}$ ).
- (b) Two physical parameters which can be observed in the field. These are the topography which can be fitted well in the model, and the depth of entrainment, fixed by the user, who knows the field situation. He can test many different values for the depth of entrainment.

The experimental site at Lautaret (Eybert-Bérard and others, 1978) has enabled us to measure velocities and specific mass as a function of time and at a given point for three avalanches. Measurement of front velocities by means of high-speed stereo-photogrammetry has been planned for the winter of 1978-79. All these factors should make it possible to examine the numerical model, and, we hope, to improve it in such a way that it becomes an increasingly satisfactory answer to the needs which we reviewed in the introduction to this paper.

*MS. received 7 September 1978 and in revised form 29 November 1979*

## REFERENCES

- Eybert-Bérard, A., and others. 1978. Mesures dynamiques dans l'avalanche: résultats expérimentaux du Col de Lautaret (1972-1978), par A. Eybert-Bérard, P. Perroud, G. Brugnot, R. Mura, L. Rey. (*In Comptes rendus. Deuxième rencontre internationale sur la neige et les avalanches, 12-13 et 14 avril 1978, Grenoble, France.* [Grenoble], Association Nationale pour l'Étude de la Neige et des Avalanches, p. 203-24.)
- Hopfinger, E. J., and Tochon-Danguy, J.-C. 1977. A model study of powder-snow avalanches. *Journal of Glaciology*, Vol. 19, No. 81, p. 343-56.
- Kozik, S. M. 1962. *Raschët dvizheniya snezhnykh lavin* [Calculation of snow avalanches]. Leningrad, Gidrometeoizdat.
- Mahmood, K., and Yevjevich, V., ed. 1975. *Unsteady flow in open channels*. Fort Collins, Colorado, Water Resources Publications. 3 vols.
- Samoylov, V. A. 1976. Stereofotogrammetricheskaya s'yemka dvizhushchikhsya lavin v Khibinakh [Stereo-photogrammetric surveys of avalanches in the Khibins]. *Materialy Glyatsiologicheskikh Issledovaniy. Khronika. Obsuzhdeniya*, Vyp. 28, p. 128-37.
- Voellmy, A. 1955. Über die Zerstörungskraft von Lawinen. *Schweizerische Bauzeitung*, Jahrg. 73, Ht. 12, p. 159-62; Ht. 15, p. 212-17; Ht. 17, p. 246-49; Ht. 19, p. 280-85.